

Uncertainty quantification of the diffuse sound field assumption in structure-borne sound radiation predictions

Edwin P.B. REYNDERS, Pengchao WANG, Geert LOMBAERT and Cédric VAN HOORICKX

KU Leuven, Department of Civil Engineering, Belgium, edwin.reynders@kuleuven.be

Abstract

When predicting the radiation of structure-borne sound into a room, it is often assumed that the generated sound field is diffuse. A diffuse field is by definition a random field: it represents a conceptual ensemble of rooms with the same volume and total absorption, but otherwise any possible arrangement of boundaries and small objects that scatter incoming sound waves. Adopting a diffuse sound field model therefore inherently introduces uncertainty on the computed results. This uncertainty can be important, especially at the lower frequency end of the spectrum. In this work, practical formulas are derived for predicting not only the mean, but also the variance of energetic level quantities, such as the band-integrated spatially averaged sound pressure level, in a diffuse sound field caused by a mechanically excited structure. The formulas are first validated in a simulation study, and then applied for predicting the sound pressure level in a room caused by impact excitation of a plate. Both the average sound pressure level and its standard deviation can be well predicted.

Keywords: Uncertainty quantification, diffuse sound field, structure-borne sound.

1 INTRODUCTION

When predicting the sound energy that is radiated by a vibrating structure into a room, the radiated sound field is usually taken to be diffuse, which means that it is a random field, composed of a large number of statistically independent plane waves, the spatial phase of which is uniformly distributed and independent from the amplitude [1]. The randomness is caused by uncertainty regarding wave scattering inside and at the boundaries of the room, either because of a lack of information, or because the wave scattering is not modeled in detail. The higher the frequency, the more sensitive the harmonic (i.e., pure tone) sound pressure at a specific point in the room becomes to such wave scattering. Since a diffuse field represents a state of maximum uncertainty (termed maximum entropy) due to wave scattering [7], it can accurately represent the state of knowledge regarding the sound field in the receiver room from a certain frequency onwards. Below this frequency, the diffuse field model will over-estimate the uncertainty caused by random wave scattering.

It is also known that the variance of the total sound energy across the random ensemble representing the diffuse field decreases with increasing modal overlap factor. Since the modal overlap factor increases with frequency, the mean total energy of the random ensemble will be close to the total energy in any particular member of the ensemble at high frequencies, so at high frequencies, diffuse fields behave essentially as deterministic, and they are often treated as such in technical acoustics. At low frequencies however, considerable variation can occur when comparing the mean total sound energy of a diffuse room model with the total sound energy for one particular member of the random ensemble.

It would therefore be desirable to quantify the uncertainty that is inherent in the diffuse sound energy as a function of frequency. Based on this uncertainty information, the analyst could then estimate, for a given vibrating structure, by how much the radiated sound energy could vary between various receiver rooms with the same gross properties. Or when a single receiver room is of interest, the analyst could then estimate from which frequency onwards taking the mean, nominal diffuse sound energy is sufficiently accurate.

The purpose of the present paper is precisely to deliver a method for quantifying the uncertainty of structure-borne sound predictions that is inherently present in the diffuse field assumption. This will be based on insights from fundamental physics that have led to diffuse field variance formulas which can be used in engineering



acoustics [4, 3]. A first contribution of the present work is that these results are complemented with the derivation of variance formulas for level quantities such as the spatially averaged band-integrated sound pressure level. A second contribution lies in the numerical and experimental validation of the proposed method.

2 PREDICTING THE VIBRATION FIELD OF THE RADIATING STRUCTURE

For simplicity, it will be assumed that the vibration field of the radiating structure depends on the direct mechanical excitation and possibly also on radiation damping, but not on diffuse sound pressure loading. The prediction of the radiated sound energy then starts with the prediction of the displacement field of the sound radiating structure, such as a floor in a building. If excitation of the structure is harmonic at frequency ω , then the displacement field $\mathbf{u}(\mathbf{x}, t)$ at position \mathbf{x} and time t can be expressed as $\mathbf{u}(\mathbf{x}, t) = \text{Re}(\mathbf{u}(\mathbf{x}, \omega)e^{i\omega t})$, where the complex vector $\mathbf{u}(\mathbf{x}, \omega)$ is termed the phasor. This phasor notation is used throughout the present and the next section. It can be easily generalized towards stationary excitation. It is assumed that the radiating structure has finite size, and that $\mathbf{u}(\mathbf{x}, \omega)$ can be accurately represented with a finite number N of modal (or generalized) displacements, which are gathered in a vector $\mathbf{q} \in \mathbb{C}^N$. If additionally the mechanical excitation of the structure is known, the modal displacements can be computed from

$$\mathbf{D}(\omega)\mathbf{q}(\omega) = \mathbf{f}(\omega), \quad (1)$$

where $\mathbf{D}(\omega) \in \mathbb{C}^{N \times N}$ represents the dynamic stiffness matrix of the structure in modal coordinates, and $\mathbf{f}(\omega) \in \mathbb{C}^N$ the vector of modal forces. The three quantities depend on frequency, but this dependency will be dropped in what follows in order not to overload the notation.

The concern in noise control is usually with energetic quantities, such as the vibrational cross-spectrum

$$\mathbf{S}_{qq} := \mathbf{q}\mathbf{q}^H, \quad (2)$$

where the superscript H denotes Hermitian (or complex conjugate) transpose. From Eq. (1), the response cross-spectrum relates to the force cross-spectrum via

$$\mathbf{S}_{qq} = \mathbf{D}\mathbf{S}_{ff}\mathbf{D}^{-H}. \quad (3)$$

3 PREDICTING THE RADIATED SOUND ENERGY

In stationary conditions, the time-averaged harmonic net acoustic power that is injected into the receiver room by the vibrating structure W_{in} , equals the time-averaged power that is dissipated in the room, W_{diss} . Adopting a hysteretic damping model for the receiver room then results in

$$W_{\text{in}} = W_{\text{diss}} = \omega\eta E, \quad (4)$$

where η denotes the (frequency-dependent) loss factor of the receiver room, and E the total time-averaged acoustic energy in the receiver room, which is the quantity of interest. In order to compute the input power W_{in} , the reaction forces that are applied onto the structure by the acoustic pressure resulting from the structure's movement \mathbf{q} , are determined. These forces are split into forces caused by the direct sound field, \mathbf{f}_{dir} , and the forces caused by the reverberant sound field, \mathbf{f}_{rev} . The input power can then be expressed as the sum of the input powers to the direct and reverberant fields:

$$W_{\text{in}} = W_{\text{in,dir}} + W_{\text{in,rev}} = \frac{1}{2}\text{Re}(i\omega\mathbf{q}^H(\mathbf{f}_{\text{dir}} + \mathbf{f}_{\text{rev}})). \quad (5)$$

The direct field is the sound field that would occur in the absence of any diffuse reflections or scattering, i.e., the sound field that would occur when the structure would be embedded in an infinite planar baffle and radiate into an acoustic halfspace. For planar structures, this sound field can be obtained by evaluating the Rayleigh

integral [2]. The result is a linear relationship between the degrees of freedom of the structure and the loading onto the structure caused by the sound pressure of the direct field, \mathbf{f}_{dir} :

$$-\mathbf{D}_{\text{dir}}\mathbf{q} = \mathbf{f}_{\text{dir}}, \quad (6)$$

where \mathbf{D}_{dir} is the dynamic stiffness matrix of the direct field of the receiver room at the interface between the room and the vibrating structure. Once the direct field dynamic stiffness matrix \mathbf{D}_{dir} has been determined, the input power to the direct field can, by application of (6), be expressed as

$$W_{\text{in,dir}} = -\frac{1}{2}\text{Re}(i\omega\mathbf{q}^H\mathbf{D}_{\text{dir}}\mathbf{q}) = \frac{\omega}{2}\sum_{j,k}\text{Im}(D_{\text{dir},jk})S_{qq,jk}. \quad (7)$$

In order to proceed, the reverberant sound field is now taken to be diffuse, which means that it is a random field, composed of a large number of statistically independent plane waves, the spatial phase of which is uniformly distributed and independent from the amplitude. The central limit theorem can then be invoked, from which it follows that the complex phasor pressure amplitudes have zero mean [1, Sec. 2.2], hence $\hat{\mathbf{f}}_{\text{rev}} = \mathbf{0}$, where the hat denotes the ensemble average. The structural vibration \mathbf{q} was assumed to depend only on the structure-borne noise source \mathbf{f} (and possibly also \mathbf{f}_{dir} , if radiation damping is accounted for, i.e., if \mathbf{D}_{dir} is included in \mathbf{D}) but not on the diffuse reaction forces $\hat{\mathbf{f}}_{\text{rev}}$. It then follows from (5) that $\hat{W}_{\text{in,rev}} = 0$ and $\hat{W}_{\text{in}} = \hat{W}_{\text{in,dir}}$. Combining Eqs. (4) and (7) and taking the expected value then results in

$$\hat{E} = \frac{1}{\omega\eta}\hat{W}_{\text{in,dir}} = \frac{1}{2\eta}\sum_{j,k}\text{Im}(D_{\text{dir},jk})\hat{S}_{qq,jk}. \quad (8)$$

From this expression, the ensemble mean of the total acoustic energy in the receiver room can be determined. When the dissipation takes place primarily in the diffuse field, the damping loss factor of the receiver room can be determined from the reverberation time T or the equivalent total absorption area A . Finally, in a sound field that is composed of plane waves, such as a diffuse sound field, the spatially averaged squared sound pressure level p_{av}^2 relates to the total time-averaged acoustic energy in the room via

$$E = \int_V e(\mathbf{x})d\mathbf{x} = \frac{p_{\text{av}}^2V}{\rho_a c^2}. \quad (9)$$

From the above analysis, the mean radiated sound energy (or spatially averaged squared sound pressure) across the considered random ensemble of rooms, can be computed. For an accurate computation of the ensemble variance, the standard notion of a diffuse field should be generalized. When random wave scattering is present within the room, the natural frequencies and mode shapes are also random. Weaver [8] found that, when there is sufficient random wave scattering such that a state of maximum information entropy is reached, the statistics of the eigenvalues of the room conform to those of the eigenvalues of a Gaussian Orthogonal Ensemble (GOE) random matrix, while the mode shapes are independent Gaussian random fields. Based on this GOE definition of a diffuse field, Langley and Brown [4] were able to derive the relative variance of the input power (or, equivalently, the relative variance of the total energy or the spatially-averaged squared sound pressure) of a diffuse field under harmonic loading with a deterministic amplitude. The result of this derivation reads

$$\frac{\text{Var}[W_{\text{in}}]}{\hat{W}_{\text{in}}^2} = \frac{\text{Var}[E]}{\hat{E}^2} = \frac{\text{Var}[p_{\text{av}}^2]}{\left(\widehat{p_{\text{av}}^2}\right)^2} \approx \frac{\alpha - 1}{\pi m} + \frac{1}{(\pi m)^2}, \quad (10)$$

where m denotes the modal overlap factor of the room and α a loading factor. The approximation in Eq. (10) is accurate when $m \geq 0.2$. In the present setting, the diffuse sound field originates from a vibrating structure via an area coupling, in which case $\alpha \approx 2$.

The harmonic mean and variance of the acoustic energy due to radiation of structure-borne sound into a diffuse field can be computed from Eqs. (8) and (10), respectively. This diffuse sound energy has a lognormal probability distribution at moderate and high modal overlap (typically for $m \geq 2$) [5]. This implies that the energy, when represented on a logarithmic scale, is normally distributed.

4 BAND INTEGRATION AND LEVEL QUANTITIES

In technical acoustics, it is customary to integrate energetic quantities over frequency bands. Since ensemble averaging is an additive operation, the mean band-averaged energetic quantities can be immediately obtained by integration, e.g., for the band-integrated energy E_B , one has

$$\hat{E}_B := \int_{\omega_l}^{\omega_u} \hat{E}(\omega) d\omega. \quad (11)$$

For the relative variance, the derivation that has led to (10) has been extended to yield [3]:

$$\frac{\text{Var}[E_B]}{\hat{E}_B^2} \approx \frac{\alpha - 1}{\pi m B^2} (2B \arctan(B) - \ln(1 + B^2)) + \frac{1}{(\pi m B)^2} \ln(1 + B^2), \quad \text{where } B := \frac{\omega_u - \omega_l}{\omega \eta}, \quad (12)$$

in which ω represents the nominal (or center) frequency of the band. For 1/3-octave bands, $B \approx 0.23/\eta$. In the derivation of Eq. (12), it has been assumed that damping and the load spectrum (which in the present application, boils down to the vibration spectrum S_{qq} of the radiating structure) be constant over the considered frequency band [3]. This implies that, in order for Eq. (12) to hold with good accuracy, the frequency band of integration should be sufficiently narrow.

The prediction of the variance of the band-integrated energy over wide frequency bands is an open problem. In this work, a practical solution is investigated, which consists of dividing the large band into several narrower bands that are (i) sufficiently narrow such that (12) holds with good accuracy, and (ii) sufficiently wide such that the band-integrated energies belonging to different bands are approximately statistically independent. When both conditions are satisfied, the mean and variance of the band-integrated energy for the narrower bands can be estimated from (11) and (12), thanks to condition (i). Thanks to condition (ii), the mean and variance of the integrated energy over the wide band are then obtained as

$$\hat{E}_B = \sum_j \hat{E}_{B,j} \quad \text{and} \quad \text{Var}[E_B] = \sum_j \text{Var}[E_{B,j}]. \quad (13)$$

The input power and spatially averaged squared sound pressure are usually represented on a logarithmic scale, as the sound power level L_W and the sound pressure level L_p , respectively:

$$L_W := 10 \log \frac{W_B}{W_0} \quad \text{and} \quad L_p := 10 \log \frac{p_{\text{av},B}^2}{p_0^2}, \quad (14)$$

where \log denotes the logarithm with base 10, and the reference values are chosen as $W_0 = 10^{-12} \text{ W}$ and $p_0^2 = \rho_a c W_0$. The subscript B is employed to emphasize that it usually concerns band-averaged quantities. From Sec. 3, it is clear that in a diffuse field, in input power, total energy and spatially averaged squared sound pressures all have the same relative variance, and that they are all approximately lognormally distributed. If this also holds for the band-averaged quantities, then the levels are normally distributed, with mean values

$$\hat{L}_W = 10 \log \frac{\hat{W}_B}{W_0} - \frac{C}{2} \quad \text{and} \quad \hat{L}_p = 10 \log \widehat{\frac{p_{\text{av},B}^2}{p_0^2}} - \frac{C}{2}, \quad (15)$$

and variances

$$\text{Var}(L_W) = \text{Var}(L_p) = \frac{10C}{\ln 10}, \quad \text{and where} \quad C := 10 \log \left(1 + \frac{\text{Var}[E_B]}{\hat{E}_B^2} \right). \quad (16)$$

From this analysis, two remarkable conclusions can be drawn: (i) the variances of all energetic levels (sound power level, sound pressure level, etc.) are the same, and (ii) the mean of an energetic level is not simply the level of the mean energetic quantity, but the error by neglecting the additional term will be smaller than 1 dB as long as the relative variance of the band-averaged energy will be smaller than 0.6.

5 NUMERICAL VERIFICATION

In this section, the foregoing theory is verified with a numerical experiment. The aim is to compute the sound pressure level that is radiated into a room by a concrete floor, which is in its turn excited by a point load. The room has a width of $l_x = 4.15\text{m}$, a length of $l_y = 5.10\text{m}$, and a height of $l_z = 4.12\text{m}$. The concrete floor on top of the room has a width of $L_x = 4.15\text{m}$, a length of $L_y = 5.10\text{m}$, and a thickness of $t = 0.10\text{m}$. The point load is applied in the vertical direction, at a distance of 1.15m from the nearest long edge and 2.10m from the nearest short edge of the floor. Its Fourier transform is constant, with an amplitude of 1N/Hz and zero phase. The concrete has a density of $\rho = 2350\text{kg/m}^3$, a Young's modulus of 40GPa , and a Poisson's ratio of 0.2 . The sound speed in the room is $c = 343\text{m/s}$, the air density is $\rho_a = 1.2\text{kg/m}^3$ and the reverberation time is $T = 1.5\text{s}$.

The rooms have a random acoustic mass distribution in the sense that a total of $N_m = 30$ point air pockets (or acoustic point masses) are distributed at random locations within each room. The air pockets are highly idealized models for small wave scatterers in the room, in the same way as point masses would be highly idealized models for small wave scatterers on a plate. Each air pocket has 0.4% of the total acoustic mass V/c^2 of the room. The probability distribution of the location of each air pocket is uniform throughout the entire room, and the locations of the air pockets are statistically independent. The total number of air pockets and their individual acoustic mass are chosen arbitrarily; the important point is that, from a certain frequency onwards, the randomness introduced by the wave scatterers reaches a state of maximum information entropy, which conforms to a diffuse field [6].

The floor is modeled deterministically, in line with Sec. 2. In particular, the floor is taken to be a homogeneous, linear elastic, simply supported thin plate with hysteretic damping. Its in-vacuo natural frequencies and mode shapes are then known in closed form, so the quantities \mathbf{D} and \mathbf{f} which appear in Eq. (1) can be computed analytically.

Two stochastic models for the room are constructed. The first room model is a detailed model, in which both the point air pockets and the modal behavior of the room are modeled in detail. This is achieved with an assumed-modes model, in which the hard-walled room modes are taken as basis functions. Realizations of the random room are computed by fixing the positions of the point air pockets with a random number generator. This process is repeated to generate a Monte Carlo ensemble of 1000 realizations of the sound field. The second room model is a diffuse field model that is constructed according to Sec. 3. In this model, the random wave scattering caused by placing the point air pockets at random locations within the room, is supposed to result in a diffuse sound field. Both room models do not only differ in the level of detail in which the room is modeled. There is also a very important difference in computation cost, since the diffuse field model is computationally much more efficient than the detailed model.

The mean and relative variance of the harmonic time-averaged total energy in the receiver room, computed with both the detailed room model and the diffuse room model, are plotted in Fig. 1a and Fig. 1b, respectively. Results from individual Monte Carlo realizations, as obtained with the detailed room model, are also displayed. At frequencies lower than about 100Hz , there are clear differences between the results obtained with the detailed and the diffuse room models. This is because in that low-frequency range, the sensitivity of the local harmonic sound field to the presence of the small random wave scatterers is relatively low, and a diffuse field model will overestimate the uncertainty caused by these random wave scatterers. However, once this sensitivity is sufficiently large, the diffuse field model is adequate: above about 100Hz , the natural frequencies of the room start to mix well across the random ensemble, resulting in a good match between the ensemble mean and variance of the energies as predicted from the detailed room model and the diffuse room model.

The mean and standard deviation of the spatially averaged sound pressure levels in 1/3-octave bands, are plotted in Fig. 1c and Fig. 1d, respectively. Not only the unweighted results are plotted, but also the A-weighted results. Since the sound pressure levels are normally distributed, confidence intervals can be directly computed from the standard deviations that are plotted in Fig. 1d; for example, a 95 % confidence interval corresponds with 4 times the standard deviation. The 95 % confidence interval corresponding to the uncertainty due to the random wave

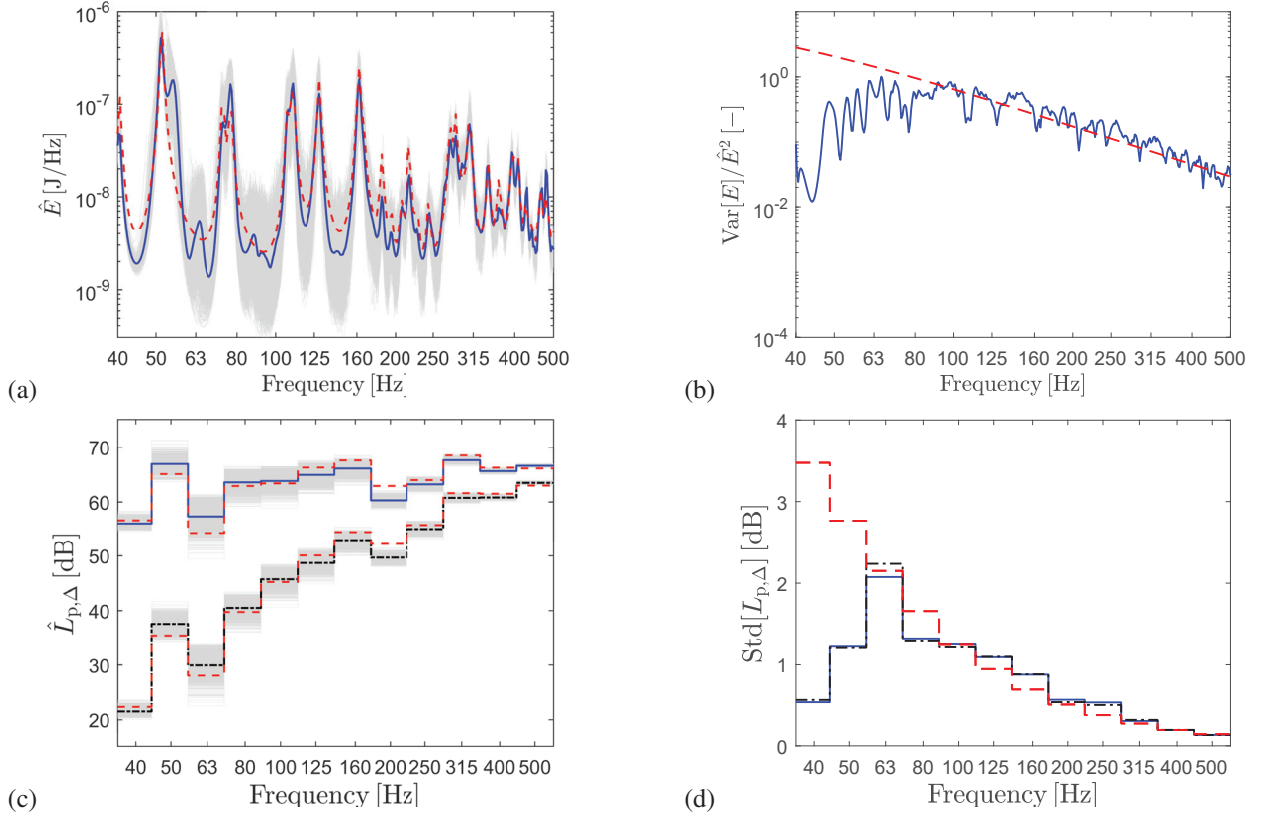


Figure 1. Response of a room with random wave scatterers, loaded by a point-excited vibrating concrete floor: (a) ensemble mean of the harmonic energy; (b) ensemble relative variance of the harmonic energy; (c) ensemble mean of the 1/3 octave band-integrated sound pressure level; (d) ensemble standard deviation of the 1/3 octave band-integrated sound pressure level. Thick solid blue lines: detailed room model statistics; thick dashed red lines: diffuse room model statistics. In plots (a,c), the results from individual Monte Carlo realizations are additionally displayed by means of thin gray lines. All results are presented without frequency weighting, except in plots (c,d), where results for A weighting are also included; the detailed room model statistics with A weighting are then represented with thick dash-dotted black lines.

scattering (and causing a diffuse field) is larger than 1dB for all 1/3-octave bands below 400Hz.

Finally, Table 1 contains the overall band-integrated unweighted (or Z-weighted) and A-weighted mean sound pressure levels and their standard deviations, as obtained from the Monte Carlo data for the detailed room model, and from Eqs. (13), (15) and (16) for the diffuse field model. On overall, the mean and the standard deviation as predicted by both models agree very well. There is a slight difference between both models for the standard deviation without weighting, because the sound pressure levels at the lowest frequencies then contribute importantly to the global response, and their uncertainty is overestimated with the diffuse field model. This increased uncertainty is the price that is paid when employing diffuse field models at low frequencies.

6 EXPERIMENTAL CASE STUDY

In this section, the foregoing methodology is demonstrated and validated by predicting and measuring the sound that is generated by a polymethyl metacrylate (PMMA) panel when impacted by a known hammer force. The

Table 1. Response of a room with random wave scatterers, loaded by a vibrating concrete floor: comparison between the mean and standard deviation of the band-integrated sound pressure levels over the entire frequency range of interest (35-560 Hz), as obtained from the detailed room model and the diffuse room model.

weighting	$\hat{L}_{p,\text{detailed}}$	$\hat{L}_{p,\text{diffuse}}$	$\sigma(L_{p,\text{detailed}})$	$\sigma(L_{p,\text{diffuse}})$
Z [dB]	75.5	75.8	0.24	0.37
A [dB(A)]	67.3	67.6	0.11	0.11

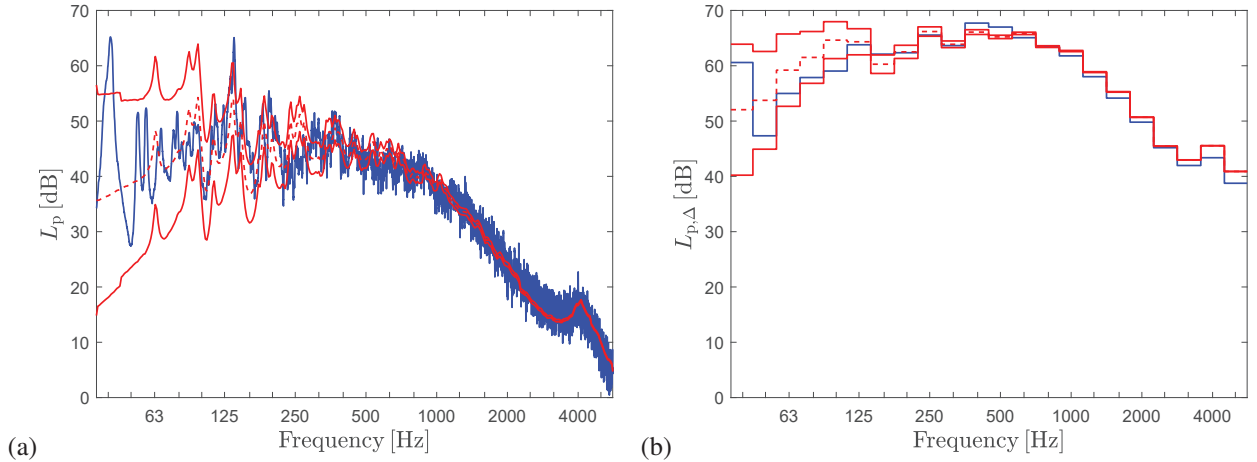


Figure 2. Sound pressure level due to sound radiation by a PMMA panel that is excited by repeated hammer impacts at a single point: (a) harmonic values and (b) 1/3-octave band values. Solid blue lines: measurements. Dashed red lines: mean predictions; solid red lines: 95% confidence interval of the predictions.

panel was mounted in the small vertical transmission opening in the KU Leuven Laboratory of Acoustics, which measures 1.25 m by 1.5 m. The receiver room has a volume of 87 m³. In order to quantify the impact force, an instrumented impact hammer is employed as excitation device. Repetitive impacts were given at a fixed location on the plate. The squared sound pressure amplitudes are measured at 8 locations in the room and subsequently averaged in order to arrive at an estimate of the average sound pressure level. In the predictions, the sound field in the room is modeled as diffuse, with nominal values for the air density and sound speed at $\rho_a = 1.20 \text{ kg/m}^3$ and $c = 343 \text{ m/s}$, respectively. For the damping loss factor of the plate and the reverberation time of the room, measured values are employed.

A finite element model of the plate was constructed using 4-node Reissner-Mindlin shell elements. The density of the PMMA material was determined at 1260 kg/m³. For the Young's modulus and the Poisson's ratio, values of 2.4 GPa, and 0.35 were assumed, respectively. The out-of-plane movement at the plate edges was prohibited since the plate was mounted against the transmission opening of the laboratory. Additionally, since the bottom edge of the plate was resting on the bottom part of the transmission opening, the horizontal movement of this plate edge was also prohibited in the direction parallel to the edge.

The excitation consisted of repetitive hammer impacts at a single location on the plate and for a total duration of 20 s. The impact location that is considered in the present paper, was at a distance of one-third of both the horizontal and vertical edge lengths of the plate, when measured with respect to one of its corners.

Fig. 2 contains the predicted and measured sound pressure levels. At low frequencies, the harmonic results contain sharp peaks that sometimes also appear in the predicted mean sound pressure level, but sometimes not. The peaks that are predicted represent modal resonances of the PMMA panel, since these are included in

the model. Modal resonances of the particular room in which the test has been performed are not visible in the predictions since a diffuse sound field model is adopted; they are instead captured by the 95% confidence interval that is associated with the diffuse field assumption. Furthermore, it can be observed that the uncertainty that is due to the diffuse field assumption is very large at the lowest frequencies, but it rapidly decreases with increasing frequency: in 1/3-octave bands, the width of the related 95% confidence interval drops below 5 dB at 125 Hz, and below 2 dB at 250 Hz. At higher frequencies, the uncertainties due to the diffuse field assumption are so small that the diffuse field model becomes essentially deterministic. At such frequencies, other sources of uncertainty will be more important than the diffuse field assumption which is investigated in the present work.

7 CONCLUSIONS

Practical, closed-form formulas have been derived for predicting not only the mean, but also the variance of energetic level quantities, such as the band-integrated spatially averaged sound pressure level, in a diffuse sound field caused by a mechanically excited structure. The uncertainty that is accounted for is the one that is inherent in the diffuse field model. The main theoretical results are Eqs. (15-16), which make the connection between the mean and variance of the level quantities and the existing results for the relative variance of the harmonic or band-averaged total energy. For simplicity, it has been assumed that the vibration field of the radiating structure depends on the direct mechanical excitation and possibly also on energy that is radiated into the direct sound field. In this case, the uncertainty of the sound pressure level which is due to the diffuse field assumption depends only on the room volume, the equivalent total absorption area of the room, the considered frequency and the integration bandwidth: the larger these quantities, the smaller the uncertainty. The formulas that are presented in the present work allow the analyst to quantify this uncertainty in a computationally cheap way, and therefore to estimate the error that is made when approximating the sound field in a specific room and at a particular frequency (band) with the mean diffuse field value. Special attention was given to the detailed numerical verification and experimental validation of the newly derived formulas.

ACKNOWLEDGMENTS

This research was funded by the European Research Council (ERC) Executive Agency, in the form of an ERC Starting Grant provided to Edwin Reynders under the Horizon 2020 framework program, project 714591 VirBACous. The financial support from the European Commission is gratefully acknowledged.

REFERENCES

- [1] K. Ebeling. Statistical properties of random wave fields. In W. Mason and R. Thurston, editors, *Physical acoustics Vol. XVII*, pages 233–310. Academic Press, Orlando, FL, 1984.
- [2] R. Langley. Numerical evaluation of the acoustic radiation from planar structures with general baffle conditions using wavelets. *Journal of the Acoustical Society of America*, 121(2):766–777, 2007.
- [3] R. Langley and A. Brown. The ensemble statistics of the band-averaged energy of a random system. *J. Sound Vib.*, 275(3–5):847–857, 2004.
- [4] R. Langley and A. Brown. The ensemble statistics of the energy of a random system subjected to harmonic excitation. *J. Sound Vib.*, 275(3–5):823–846, 2004.
- [5] R. Langley, J. Legault, J. Woodhouse, and E. Reynders. On the applicability of the lognormal distribution in random dynamical systems. *J. Sound Vib.*, 332(13):3289–3302, 2013.
- [6] R. Lyon. Needed: a new definition of diffusion. *Journal of the Acoustical Society of America*, 56(4):1300–1302, 1974.
- [7] P. Shorter and R. Langley. On the reciprocity relationship between direct field radiation and diffuse reverberant loading. *Journal of the Acoustical Society of America*, 117(1):85–95, 2005.
- [8] R. Weaver. On the ensemble variance of reverberation room transmission functions, the effect of spectral rigidity. *J. Sound Vib.*, 130(3):487–491, 1989.